Development of a roundness measuring system for microspheres

Development of a roundness measuring system for microspheres

Kuang-Chao Fan[1,2]**, Na Wang**[1]**, Zhi-Wei Wang**[1] **and Hui Zhang**[1]

[1] School of Instrument Science and Opto-electronic Engineering, Hefei University of Technology, Tunxi Road 193, Heifei, 230009, People's Republic of China
[2] Department of Mechanical Engineering, National Taiwan University, l, Sec. 4, Roosevelt Road, Taipei, 10617, Taiwan

E-mail: fan@ntu.edu.tw

Abstract
In the field of micro/nano technology, microspheres are often used as the tip-ball of a measuring stylus, such as in micro/nano coordinate measuring machines (CMMs). Conventional tactile probes adopt ruby or steel balls with diameters in the range of several millimeters to 0.3 mm. For a micro-CMM, the required probing ball is as small as possible in order to be inserted into a small groove for side wall measurement. The exact diameter of the tip-ball has to be calibrated for radius compensation and its roundness error has to be qualified. A roundness measuring system for microspheres is developed in this study. Two small Michelson interferometers are designed for direct measurement of microsphere diameter from both sides, being a two-point method. By rotating the measured sphere and reading the displacement shifts of the two interferometers, the run-out of the sphere can be eliminated. The resolution of the developed system can reach 1 nm and the accuracy can reach 10 nm. Two microspheres are tested with good repeatability. This system can also be used for macrosphere measurement.

Keywords: roundness measurement, microsphere, Michelson interferometer, diameter variation

(Some figures may appear in colour only in the online journal)

1. Introduction

The coordinate measuring machine (CMM) is a versatile and widespread metrology instrument for three-dimensional (3D) measurements for macro objects. With the advent of miniaturization in mechanical, MEMS and optical products, a new demand for highly accurate dimensional measurements on micro parts is urgently required. Up to now, the limiting factors for the use of CMMs for the measurements of small object features are focused on the size of the mechanical probes and the measuring uncertainty [1]. Although a few commercial micro-CMMs are available that permit probing with small spheres, such as [2–5], these are of point-contact type that cannot provide continuous shape error of the roundness of a small ball. Most probing balls used in micro-CMMs are with a diameter ranging from 1 mm to 30 μm. As the probe ball gets smaller, it is impossible to reach perfect sphericity.

Only limited literatures addressed the way of roundness calibration of micro contact balls, such as [2, 6]. For macro-CMMs, the roundness of the probing ball is assumed smaller than the machine accuracy so that only the ball radius at the contact point has to be compensated in either the touch-trigger mode or the contact-scanning mode [7, 8]. For micro-CMMs, however, the accuracy of the machine is at submicron or nanometer level, and the actual dimension and roundness of the ball becomes important.

Most of the commercially available ball tips are made of ruby because of its good anti-wear characteristics. However, the ruby balls are expensive and it is also difficult to obtain ruby balls with diameters less than 100 μm. The fabrication of micro-ball styluses can be made by two processes. One is to directly melt the stylus tip by electrical discharge energy and let it form a spherical shape during solidification, based on the phenomenon of material-free expansion. The achievable ball

diameter is dependent on the stylus tip diameter. The micro gravity effect has to be compensated for or the tip droplet shape will be formed. Hidaka formed a glass tip-ball with a diameter of 30 μm [9]. Sheu formed a tungsten tip-ball with a diameter of 40 μm [10]. Ji *et al* formed a fiber tip-ball with a diameter of about 250 μm [11]. Fan *et al* formed some fiber tip-balls with a diameter of about 300 μm [12, 13]. The other method is to glue a commercially available glass micro sphere onto a stylus tip assisted by a positioning stage. Shimizu *et al* used a tapered glass tube or a stainless shaft to produce micro-ball styluses for scanning-type surface form metrology [14]. The adopted tip-ball ranges from 50 to 10 μm. The center offset of the ball from the shaft is, however, 1 μm and the roundness of the ball is unknown. These errors will affect the radius compensation results.

For roundness measurement in general, there are two basic types of commercially high precision roundness measuring instruments, namely the rotating spindle type and the turntable type. Unfortunately, the probe diameters are of the millimeter scale, such as Talyrond 365, with which it is not easy to contact a small sphere with a diameter of micrometers. To achieve the measuring capability, some solutions have been proposed in recent years, such as digital image analysis [15, 16] and the AFM-combined rotary air bearing method [17]. The image method has low resolution due to the diffraction limit. The AFM method cannot separate the run-out error of the spindle. The use of a CMM is also possible to measure the roundness of the object, but is still limited to the ball's diameter. Küng *et al* achieved sphere calibration of 1 mm in diameter using a developed ultraprecision micro-CMM for traceable measurement for small parts with nanometer accuracy [2]. The calibration results on three 1 mm calibration spheres showed excellent repeatability with the standard deviation at one given point being usually less than 4 nm. They also showed the ISO 10360 scanning acceptance tests on a 1 mm sapphire sphere with excellent standard deviation in measured roundness and any given location, all less than 5 nm. This is an important report on roundness measurement so far in the world. It is, however, a highly costly and time consuming method, and there is no report for spheres in the micrometer dimension.

It is known that the influence of the accuracy of the microsphere on measurement errors on CMM is also an important issue. Michihata *et al* developed the nano-probe system based on the laser-trapping technique [18, 19]. On a nano-CMM of 50 nm measuring accuracy, the repeatability ($k = 2$) of a flat surface sensing with the fixed contact point of the probe ball is ± 64 nm. However, the total measurement uncertainty on 3D objects with a glass sphere with changed contact points of the tip-ball of 553 μm diameter was about 335 nm among which the probe contributes 128 nm. It can be seen that the roundness of the tip-ball indeed increases the measurement errors on CMM.

Kühnel *et al* set up a non-tactile high-precision turntable type inner roundness measurement system of hollow cylinders with two laser interferometers that measure the two 180° shifted radial roundness deviations of the ring gauge [20]. It deals with only the inner roundness measurement of large
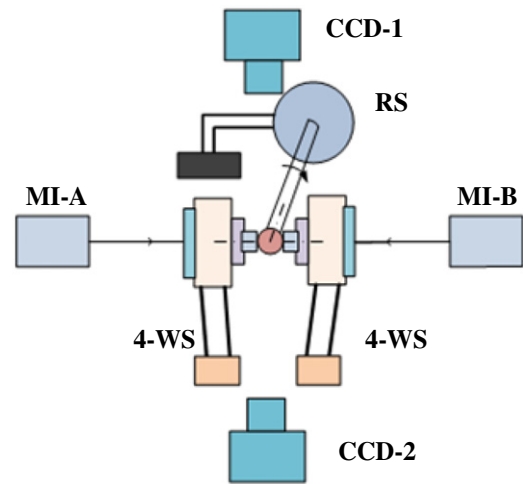

Figure 1. System configuration of the roundness tester.

cylindrical parts. Although the influence of the offset of the measured part to the rotating center has been investigated, the run-out of the turntable was not considered.

The geometrical product specifications of roundness can be found in ISO 12181-1, which defines the radial deviation of a roundness profile from the reference circle [22]. In this study, a new method is developed for the roundness measurement of microspheres. It is based on the two-point method for error separation given in the NBSIR 79–1758 standard [23]. This proposed method is similar to [20] in the way of using two laser interferometers for direct measurements of two 180°-shifted points. Each point movement during rotation is detected by a developed miniature Michelson interferometer (MI). Not only can the resolution reach 1 nm but also the run-out can be removed. Due to the accuracy limitation of the developed system, current progress only presents the roundness evaluation by diameter variation around the measured circle. Details are described in the following sections.

2. Principle of roundness measurement

2.1. Measurement principle

The system configuration of the proposed roundness measurement is shown in figure 1. The tested small ball is bonded on a thin stylus, which is clamped by a rotary stage (RS). Two small side mirrors and structure are pushed to make contact with the tested ball with a preloaded four-wire spring (4-WS) on each side. When rotating the tested ball, its radial change as well as run-out will push two side mirrors, whose motions can be detected by the corresponding laser interferometers of Michelson type (MI), respectively. Since the ball and mirrors are too small to be viewed by human eyes, two microscope CCD cameras mounted on the top and front are employed to enlarge the images for positioning alignment in three linear and two angular axes. Figure 2(*a*) shows the situation when two side mirrors are contacted in good alignment. Figure 2(*b*) depicts the situation when the side mirror B is moved away to allow the tested ball to be
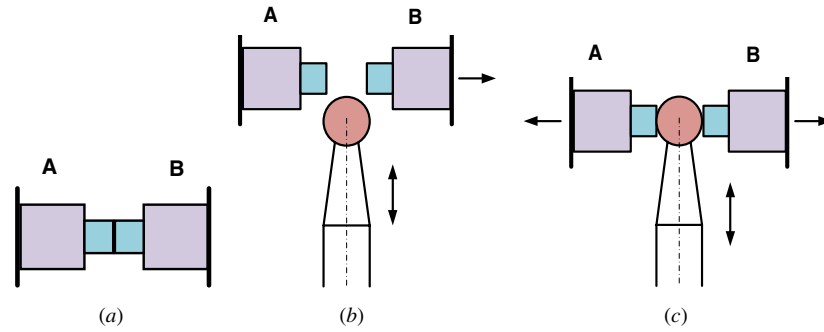
Figure 2. Positioning the tested ball: (*a*) no engagement, (*b*) open B and insert ball, (*c*) final position.

inserted. Figure 2(*c*) shows the final position when the tested ball is aligned with the common central line of the laser interferometer.

When the tested ball is not engaged, the two side mirrors are in the contact position with central lines aligned. The readings of both MIs are reset. When the tested ball is moved to the final position, the sum of the two interferometer readings is the diameter of the ball at this initial position. When rotating the ball, its run-out is automatically compensated by the two readings. At any rotating angle θ, the diameter of the tested ball D can be read as the sum of the left interferometer reading T_a and the right interferometer reading T_b:

$$D(\theta) = T_a(\theta) + T_b(\theta). \tag{1}$$

Completing a one-half cycle rotation at given incremental steps, the diameter variation of the tested ball can be obtained. The roundness is defined as the maximum to minimum of the measured diameters. It is noted that the side mirrors must be very small and thin, otherwise the camera image will be blocked. The details will be expressed in section 3.

2.2. Principle of the Michelson interferometer

The MI is a well known length measurement instrument. It normally adopts a He–Ne laser tube as the light source for long coherence length but the size cannot be reduced to small lengths. Büchner and Jäger developed a miniature laser interferometer through a coupled fiber to the He–Ne laser [24]. The portable laser head is very compact and good for use as a position feedback sensor in precision machines. The cost is, however, expensive, considering that the actual measurement length of small sphere roundness is relatively short, being in the micrometer range. The proposed system directly uses a laser diode as the light source with prior wavelength calibration.

The optical system of the developed miniature MI is illustrated in figure 3. A partially polarized laser beam of about 635 nm wavelength from the laser diode LD impinges on the polarizing beam splitter PBS1 and is split into two beams: the transmitted P-beam and the reflected S-beam. The intensity balance of these two beams can be adjusted by rotating the laser diode. The S-beam passes through Q1 and reflects back by the reference mirror, and P-beam passes through Q2 and is reflected back by the object moving mirror (OM). The quarter waveplates Q1 and Q2 prevent the beams from going back into the laser diode, for each polarization state will be
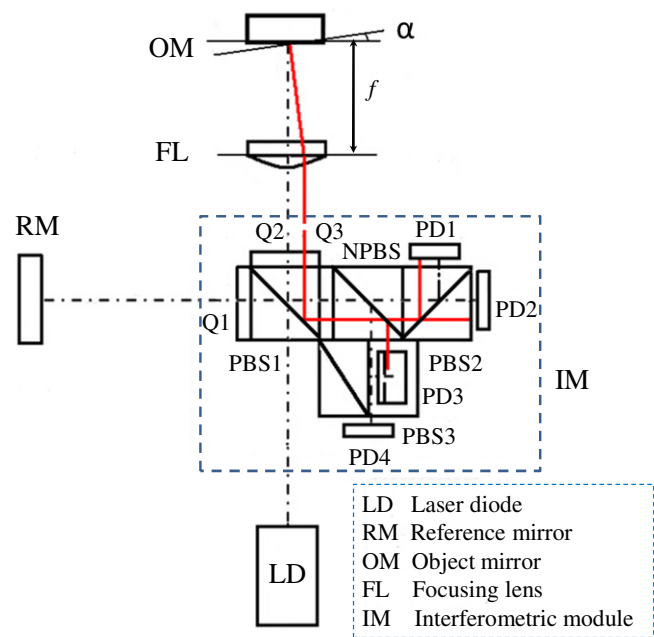

Figure 3. Optical configuration of the Michelson interferometer.

changed by 90° after passing a quarter waveplate twice. The two beams are combined at PBS1 and converted into left and right circularly polarized beams by Q3, respectively. With the phase shift module composed of NPBS, PBS2 and PBS3, four interference fringes with 90° phase shift to each other can be detected by photodetectors PD1–PD4, respectively. During the movement of OM, the interference fringe will have a phase shift proportional to the displacement of movement. In addition, considering that the OM may tilt a slight angle α due to the inevitable alignment error of the ball and the mirrors in assembly resulting in an additional optical path difference, a focus lens FL is thus placed between the OM and Q2. Its purpose is to reduce the generated optical path difference and the lateral shift of the reflected beam from OM, as shown in figure 3.

The light intensity on each photodetector can be obtained as:

$$I_{PD1} = |E_{PD1}|^2 = E_0^2 \left(1 + \cos\left(\Delta\omega t + k\Delta r + \frac{\pi}{2}\right)\right), \tag{2}$$

$$I_{PD2} = |E_{PD2}|^2 = E_0^2 \left(1 + \cos\left(\Delta\omega t + k\Delta r - \frac{\pi}{2}\right)\right), \tag{3}$$
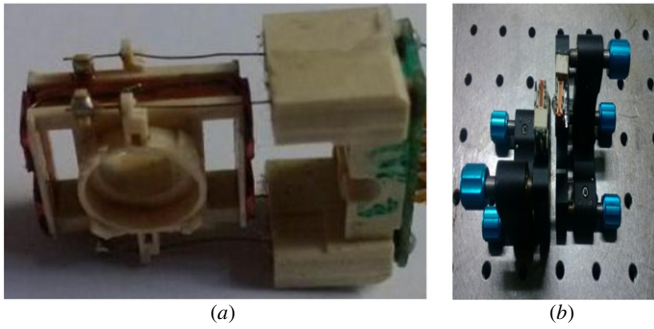
Figure 4. The elastic mechanism: (*a*) the disassembled VCM mechanism, (*b*) assembled into adjustable stages.

$$I_{PD3} = |E_{PD3}|^2 = E_0^2 \left(1 + \cos\left(\Delta\omega t + k\Delta r + \pi\right)\right), \quad (4)$$

$$I_{PD4} = |E_{PD4}|^2 = E_0^2 \left(1 + \cos\left(\Delta\omega t + k\Delta r\right)\right). \quad (5)$$

Let $\Delta\Phi = \Delta\omega t + k\Delta r$, two sinusoidal waveforms in $90°$ phase shift can be obtained:

$$S_1 = I_{PD1} - I_{PD2} = 2E_0^2 \sin\Delta\Phi, \quad (6)$$

$$S_2 = I_{PD3} - I_{PD4} = 2E_0^2 \cos\Delta\Phi. \quad (7)$$

It is clearly seen that the signal's dc offset can be effectively eliminated by the difference of equations of (2) and (3) for the sine term, and of (4) and (5) for the cosine term respectively. The residual phase is determined by

$$\Delta\Phi = k\Delta r = \tan^{-1}\left(\frac{S_1}{S_2}\right). \quad (8)$$

The displacement of the moving mirror is calculated by the number of interfering waves (N) and the residual phases at the start-up and end positions, respectively,

$$d = \left[\frac{\Delta\Phi_{End} - \Delta\Phi_{Start}}{2\pi} + N\right] \times \frac{\lambda}{2}. \quad (9)$$

It is noted that the actual wavelength of the laser diode has to be calibrated, which will be expressed in section 4.

3. Construction of the roundness measurement system

The developed roundness tester for small balls consists of three modules, namely the elastic mechanism for fixing the side ball and the reflection mirror, the adjustable stage to align the two side mirrors, the MI for measuring the mirror movement and the rotation module to drive the tested ball. Details are described below.

3.1. The elastic mechanism

The elastic mechanism is used to support the side mirrors and the reflection mirror shown in figure 1. The part of the 4-WS mechanism is directly disassembled from the voice coil motor (VCM) of a DVD pickup head. Figure 4(*a*) shows the photo of the VCM mechanism with 4-WS support. The object mirror used for reflecting the laser beam is mounted onto the front ring of the moving mass of the spring mechanism. To the other side of the moving mass will be attached a miniature mirror. Figure 4(*b*) shows the photo of two elastic mechanisms mounted onto two 3-DOF adjustable stages, respectively. Each stage provides two angles and one linear fine motion of the elastic mechanism so as to align the two side balls perfectly as required by figure 2(*a*).

The two-sided mirrors were previously fabricated by the MEMS process for the use in optical switches [25]. Each mirror was made on the wafer substrate with dimensions of 2×1 mm^2 and 0.5 mm thickness, as shown in figure 5(*a*). The surface was coated with Cr/Au by deposition. Figure 5(*b*) shows the surface profile of portion A, measured by AFM, with flatness error of about 5 nm only. The size and reflectivity are all good to use here.

3.2. Miniature Michelson interferometer

The developed MI has to be as small as possible because it is used as the displacement sensor of the moving mirror. All the optical components are purchased from the market with the available smallest dimension of 5 mm side length. As each part is too small to be handled, the assembly is extremely difficult either with glue bonding or optical bonding. A mechanical clamp was designed to achieve the assembly of the interferometric module required by figure 3 [26]. Figure 6(*a*) shows the photo of the developed miniature MI with dimensions of about 50 mm by 50 mm. Figure 6(*b*) shows the photo of the assembly of the elastic mechanism and the interferometer.
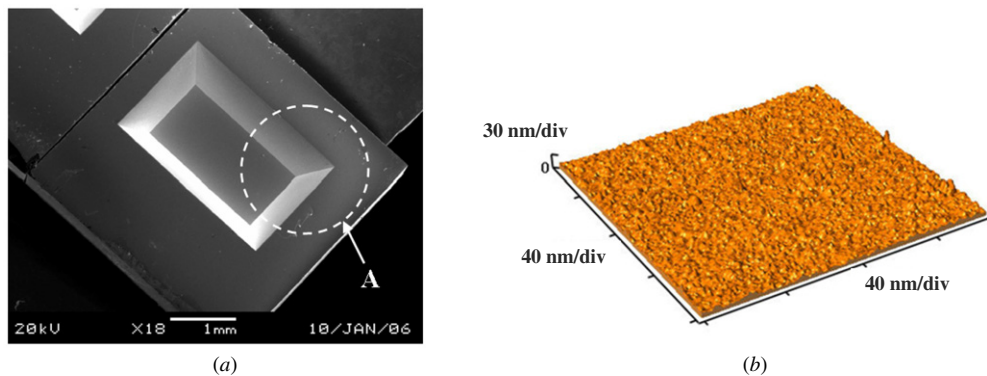

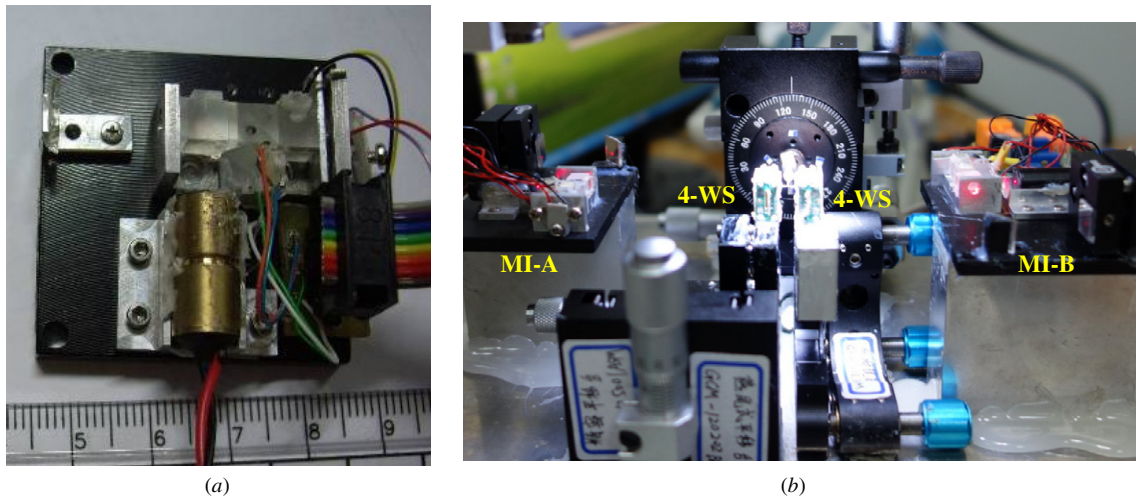**Figure 5.** Fabricated small mirror: (*a*) SEM photo, (*b*) surface profile measured by AFM.

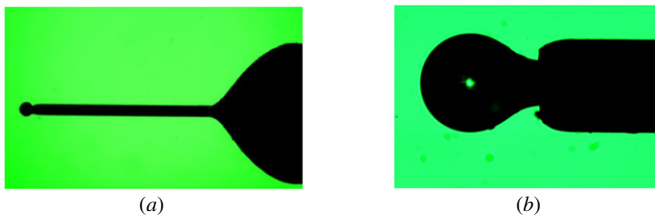**Figure 6.** (*a*) Assembled Michelson interferometer, (*b*) assembled with elastic mechanism.

Figure 7. Fabricated tip-ball stylus: (*a*) full length view, (*b*) enlarged tip end view.
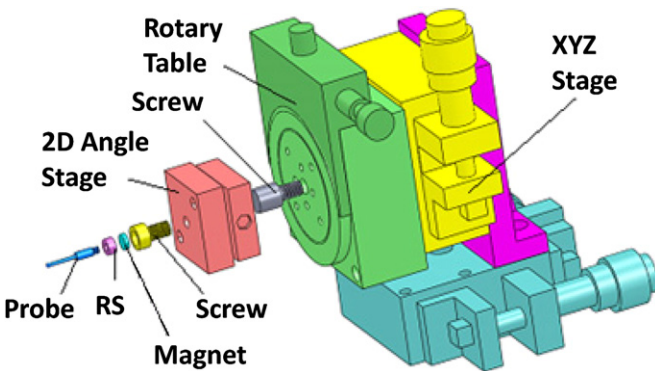

Figure 8. Design of the rotation module.

3.3. Fabrication of tip-ball stylus

The tested ball was fabricated by the arc-discharge process on an optical fiber tip with about a 300 μm tip-ball diameter [12, 13]. It is to be used as the touch probe for the micro-CMM. The fiber stem is inserted into a steel medical hypodermic needle in order to strengthen the stylus stiffness. After careful gluing, the photo of a tested tip-ball is shown in figure 7(*a*). Figure 7(*b*) is the close-up view of the tip end. The quality is good to use.

3.4. Rotation module

A manual type RS is used to drive the tip-ball stylus to any specified angle. The structure is shown in figure 8. The stylus is

screwed to a ring thread (RS), which is mounted onto a magnet plate. Through a screw the magnet is attached to a dual-axis angle stage (made of aluminum alloy), which is connected to the central hole of the RS via a second screw. The RS can be positioned by an XYZ-stage in order to position the tip-ball of the stylus between two side mirrors as illustrated in figure 2. The 2D angle stage provides pitch and yaw adjustment of the stylus, while the magnet can be tapped to finely adjust the center axis of the stylus in line with the center of the RS. It has to be pointed out that although the design consideration is thorough, there are still some errors affecting the alignment and positioning of the stylus to the rotating axis, such as the manufacturing errors of the center hole of the RS, the centering error of the tip-ball and the needle stylus, the wobble of the RS, etc. As a result, the tested microsphere will appear more or less run-out during rotation. In actual tests, the run-out of the ball is about 50 μm maximum.

3.5. The roundness measurement system

Having completed all the modules, the system was assembled with careful fine-tuning alignment. Figure 9 shows the photo of the experimental setup for the roundness test of a small tip-ball in stylus. CCD-1 is the camera lens of an optical profiler to enlarge the top view image of the rotating ball and CCD-2 is a portable microscope CCD to enlarge the front view image. The two Michelson interferometers (MI-A and MI-B) were carefully aligned in line and center to the rotating ball. Figure 10 shows the sequence of engagement of the tested ball to the center of two side mirrors, as expressed in figure 2.

4. Experiments

4.1. Calibration of the Michelson interferometer

For a laser interferometer measurement system, the attainable accuracy of measurement in the air mainly depends on the accuracy of the wavelength, and the influence of the ambient temperature. The room temperature was maintained at 22 $\pm$ 1 °C, i.e. normal laboratory conditions. Output sinusoidal
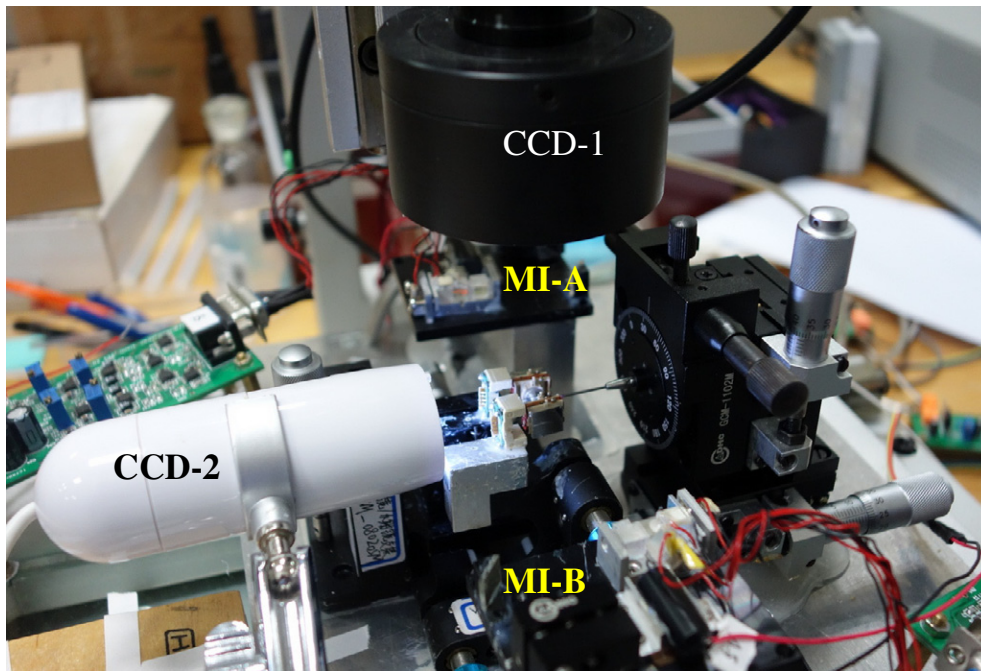
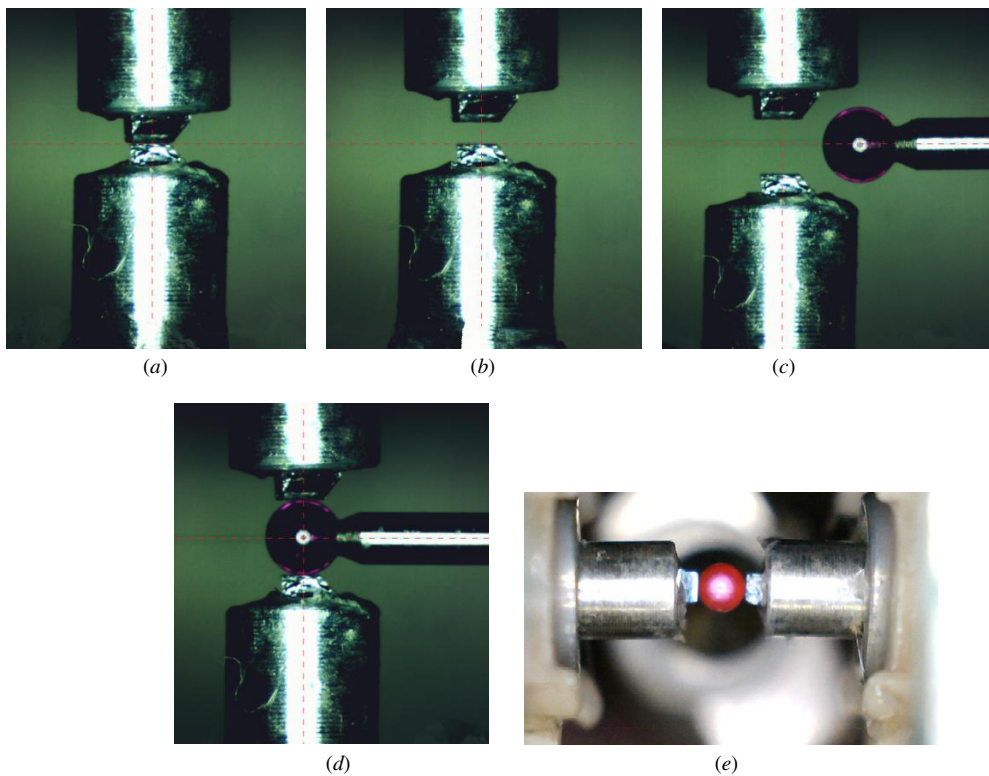**Figure 9.** Assembled roundness tester for small balls.

Figure 10. Photos of the sequence of positioning the tested ball: (*a*) two mirrors are in contact position, (*b*) mirror B is pushed out, (*c*) tested ball is moving in, (*d*) final position of top view, (*e*) final position of front view.

signals in the form of a Lissajous circle was found very good and stable under moving and stationary conditions, as shown in figure 11.

During the signal stability testing, the displacement value of the MI was recorded every 5 s, the whole test lasted for 100 min. The signal drift was less than 50 nm, as shown in figure 12. This duration is long enough to complete one roundness test.

Each MI was calibrated by a commercial Renishaw laser interferometer in order to find the exact wavelength under
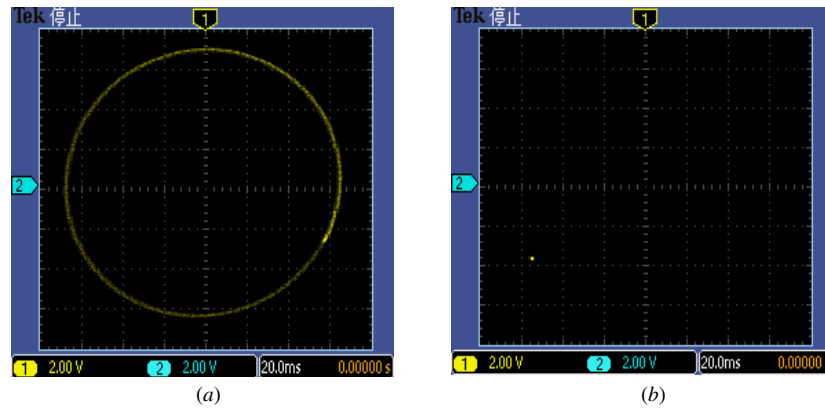
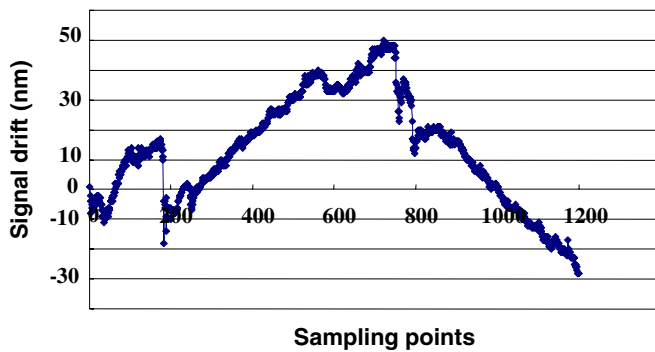**Figure 11.** Signal output of Michelson interferometer. (*a*) Signal in movement, (*b*) signal stationary.

Figure 12. Michelson interferometer signal stability testing.

Table 1. Calibration results of the two Michelson interferometers (μm).

MI-A	Renishaw	MI-B	Renishaw
−0.001	0.003	−0.001	−0.003
101.893	101.989	100.627	100.736
202.320	202.601	201.770	202.047
302.257	302.655	301.195	301.591
404.338	404.950	403.471	404.101
501.269	502.058	502.136	502.940
601.376	602.291	600.534	601.461
701.993	703.008	700.741	701.761
801.496	802.656	802.793	803.929
903.057	904.286	900.636	901.849

the controlled temperature. The two optical axes of the laser beams were adjusted to the same axis, which coincided with the motion direction of a linear stage. Moving the linear stage manually with about a 100 μm incremental step and recording both the Michelson displacement and the Renishaw interferometer readings, a list of comparison data was attained, as shown in table 1. It was found that with the use of the wavelength for the laser diode provided by the vender, i.e. 635 nm, both MIs output with shorter displacements. A linear relationship between two readings could be found by least-squares line fitting. The slope of MI-A was 1.0014 and MI-B was 1.0013. Therefore, with this calibration method, the exact wavelength of the MI was found to be 635.889 nm for MI-A and 635.826 for MI-B, which was corrected from the original 635 nm. The maximum residual after this wavelength correction process was less than 90 nm corresponding to the
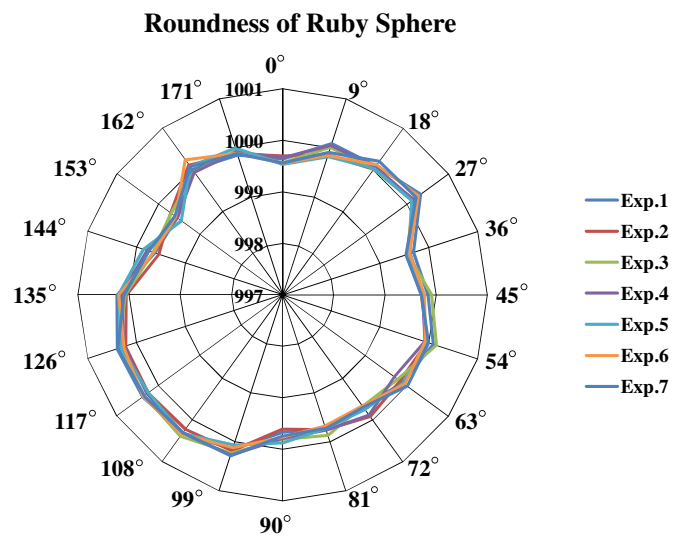

Figure 13. Measured diameter variation of the ruby sphere.

full range of 900 μm, and was only 10 nm for the short range of 5 μm. Normal roundness error of any fabricated small tip-ball will be smaller than 5 μm. The accuracy of the MI is reliable.

4.2. Roundness tests

Two tip-ball styluses were tested. The first one was a commercial ruby–ball stylus of Renishaw Co. The nominal diameter is 1 mm. The sequence of positioning the tested ball has been shown in figure 10. The stylus was rotated manually at an incremental angle of 9° by the RS. The positioning is determined by the scale reading. Figure 13 shows the measured diameter variation of a half cycle rotation of seven times. Table 2 lists the average diameter and calculated roundness error (maximum diameter variation) of each time. The diameter on average was 999.938 μm with standard deviation 17 nm. The roundness error was 0.812 μm with standard deviation 60 nm. If we look at the diameter variation at each position, figure 14 shows that the standard deviation is between 0.05–0.11 μm. The maximum uncertainty of positional diameters is larger than the uncertainty of averaged diameters. It is because the latter one has the smoothing effect. The causes of measurement uncertainty will be discussed in
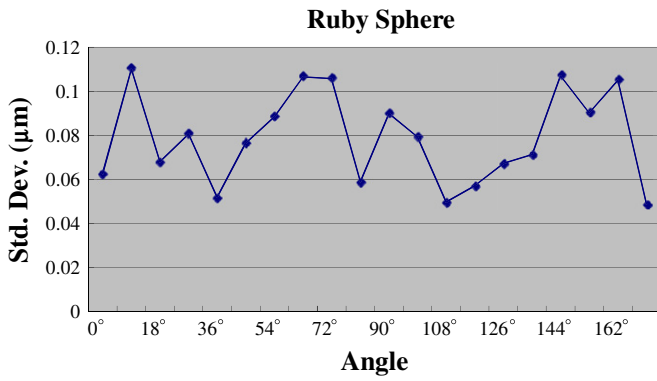
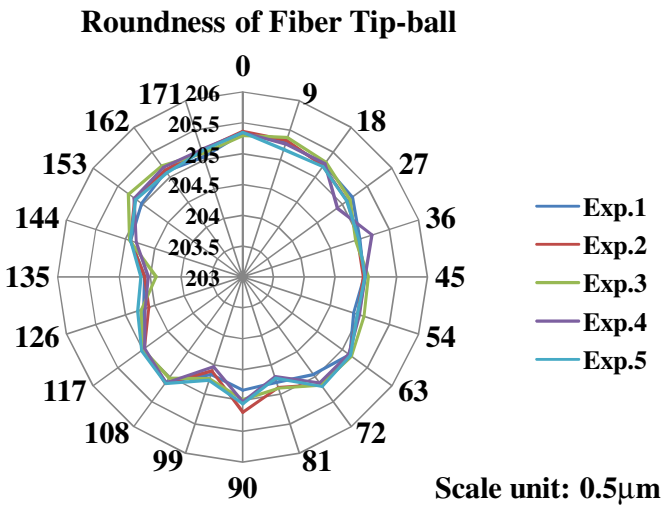**Figure 14.** Standard deviation of the measured diameter at each position.

Figure 15. Measured diameter variation of the glass fiber sphere.

Table 2. Measured data of the ruby sphere.

Time	Diameter (μm)	Roundness (μm)
1	999.9597	0.843
2	999.9092	0.7
3	999.9513	0.835
4	999.9355	0.773
5	999.9253	0.878
6	999.9365	0.806
7	999.9466	0.85
Avg.	999.9377	0.8121
σ	0.017	0.060

the next section. The second test was on a self-fabricated glass fiber tip-ball stylus with a diameter around 250 μm [12, 13]. Measured results presented in figure 15 and table 3 show the diameter on average of five times was 205.0165 μm with standard deviation 20 nm. The roundness error was 0.798 μm with standard deviation 104 nm. It is found that the smaller diameter has poorer repeatability. The random run-out of the RS is more critical to the smaller diameter tested balls.

4.3. Discussions

4.3.1. Comparison with the optical method. The optical measurement system is an image profile projector made
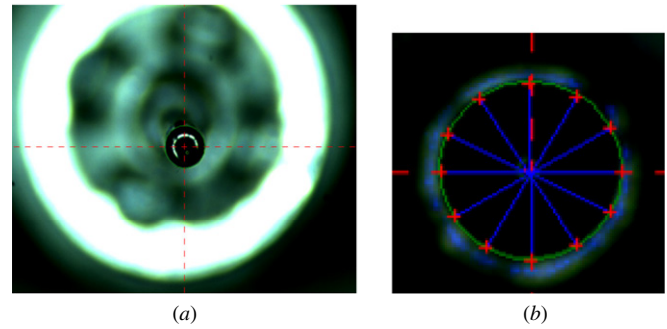

Figure 16. Sphere measurement by optical method: (*a*) improper vertical alignment, (*b*) selecting measured points after alignment.

Table 3. Measured data of the glass fiber sphere.

Time	Diameter (μm)	Roundness (μm)
1	204.9897	0.739
2	205.0255	0.775
3	205.0399	0.966
4	205.0027	0.816
5	205.0249	0.694
Avg.	205.0165	0.798
σ	0.020 054	0.104 132

by 3DFamily Co. (www.3dfamily.com) model number MUMA200, for small dimensional measurements. It provides roundness measurement software which can detect the edge point nearest to the cursor point the operator has specified by mouse clicking manually. The indicated optical resolution is 1 μm. As indicated in section 3.5 and figure 9, CCD-1 is the camera lens used in this profile project. In order to compare the same equator plane of the measured sphere, the ball tip stylus has to be set up vertically. Figure 16(*a*) shows the photo when the vertical alignment is not yet perfect, the tip-ball has significant offset to the stylus center. An elliptical shape could be measured. Figure 16(*b*) shows the enlarged image of the interested object tailored from the whole image frame when the alignment has been done to the best of manual operation, though a slight offset still could not be avoided. The '+' marks are the carefully selected edges automatically detected by the measurement software. For the ruby sphere of about 1 mm diameter, the measured diameter was 1000.19 μm on average with standard deviation 0.1 μm and the calculated roundness error was 0.88 μm on average with standard deviation 0.55 μm. For the fiber sphere, the measured diameter was 205.18 μm on average with standard deviation 0.36 μm and the calculated roundness error was 1.54 μm on average with standard deviation 1.02 μm. It is seen that all parameters measured by the optical method are larger than the developed method and the smaller the diameter the worse the repeatability. The problem could be the difficulty in perfect vertical alignment of the stylus. It is also believed that the valid digital number of the optical image is only 1 μm, all digits after it are regarded as meaningless. Most importantly, the characteristic shape of the sphere can be reproduced much better by the developed system.

4.3.2. Influence of the contact force. The contact force of the sphere and the side plane is reacted by the WS of the VCM. Our previous study on the mechanical system of VCM showed the spring constant of the used VCM (taken from a DVD pickup head made by Sony, model number KHM 220) is 26.74 N m^{-1} [26]. The contact force for a maximum 100 μm of movement is estimated to be about 2.7 mN. As the contact force is small and the contact planes are super flat, as shown in figure 5, the sphere will not be damaged during measurement.

4.3.3. Uncertainty estimation. The main purpose of this study is to propose a new measuring technique to evaluate the roundness of microspheres by two interferometers so that the characteristic shape around the circle can be found clearly. This is important to the radius compensation to nanometer level when the sphere is used as a tactile probe in micro-CMM. Since the current system is composed of developed modules, namely the miniature interferometer, elastic mechanism, manual type rotary table, manual type adjustable stages and holding fixtures, the measurement uncertainty is still large. It is expected that if the whole system could be produced of more accurate modules to become a useful instrument, the measurement uncertainty would be reduced significantly as reported by [2] and [20]. For the current system, the measurement uncertainty could be caused by the following sources:

(1) The wobble of the RS, which was measured to be about ± 50 μm with maximum standard deviation of about 20 μm for five times near the edge by a dial indicator. This amount of non-repeatability, together with the tilt and center offset of the stylus mounting, will create significant run-out error and corresponding uncertainty of the sphere during rotation. The uncertainty of measured roundness error caused by this source is estimated to be about 60 nm.
(2) The drifts of the two laser interferometers, which were measured to be about 50 nm each over 100 min, similar to the result of figure 11. The uncertainty of simultaneous readings of two interferometers is estimated to be about 80 nm.
(3) The environmental variation, which was approximately ± 0.5 °C in temperature variation around the measuring system, which was mounted on a passive type air table. The uncertainty of this part is estimated to be about 60 nm.
(4) The positioning error due to scale reading, which would cause uncertainty of measured diameter at different angles. The maximum angular positioning error is about two tenths of the scale unit, i.e., 0.6°. The caused uncertainty should be less than 10 nm.

Other sources, such as the alignment error of the two interferometers, the uncertainty of the spring constants of the two elastic mechanisms, the roughness of the spheres as well as the flat mirrors, etc. would not be as large as the above first three terms to the measurement uncertainty. Therefore, if the uncertainty due to the run-out, drift of laser interferometer and environmental variation could be reduced, the measuring system would be very repeatable.

4.3.4. Radial variation measurement. This is the goal of our research in order to conform to the ISO standard [22]. However, to separate the radius error from the run-out, the sphere has to be rotated by 180° for reverse measurement [23]. How to rotate the sphere without generating position offset is a challenging work. More sophisticated and accurate systems should be designed in the future.

5. Conclusions

In this study, a novel roundness measurement system has been developed for the roundness measurement of microspheres. Two small Michelson laser interferometers are also developed as the sensor module and two elastic mechanisms are designed to hold the contact points of two small mirrors. This type of two-point method directly measures the diameter and its variation of the tested sphere. The run-out error of the sphere is automatically removed. The exact wavelength of the MI can be found by comparing it with a commercial laser interferometer. The resolution of the MI is 1 nm and the accuracy could reach 10 nm for the diameter variation within 5 μm. This system is not only suitable for microspheres but also for macrospheres. This is the first report of the developed system. Current roundness error is evaluated by the diameter change. A clear characteristic shape could be seen. The measurement uncertainty is, however, still large. If the uncertainty due to run-out, drift of the laser interferometer and environmental variation could be reduced, the measuring system would be very repeatable.

In order to measure the radius variation to conform to the ISO standard, the reverse method has to be applied with the condition that the sphere remains at the same position after 180° rotation. To achieve this goal, a more sophisticated and accurate system should be designed in the future.

References

[1] Schwenke H F, Härtig F, Wendt K and Wäldele F 2001 Future challenges in co-ordinate metrology: addressing metrological problem for very small and very large parts *Proc. IDW 2001 (Knoxville, USA, 2001)* pp 1–12
[2] Küng A, Meli F and Thalmann R 2007 Ultraprecision micro-CMM using a low force 3D touch probe *Meas. Sci. Technol.* **18** 319–27
[3] Bos E J C, Delbressine F L M and Haitjema H 2004 High-accuracy CMM metrology for micro systems *VDI Berichte* **1860** 511–22
[4] Vermeulen M M P A, Rosielle P C J N and Schellekens P H J 1998 Design of a high-precision 3D-coordinate measuring machine *Ann. CIRP* **47** 447–50
[5] Weckenmann A, Peggs G and Hoffmann J 2006 Probing systems for dimensional micro- and nano-metrology *Meas. Sci. Technol.* **17** 504–9
[6] Lapik Company 2013 http://lapic.ru/eng/details/small
[7] Estler W T *et al* 1996 Error compensation for CMM touch trigger probes *Precis. Eng.* **19** 85–97

[8] Lin Y C and Sun W I 2003 Probe radius compensated by the multi-cross product method in freeform surface measurement with touch trigger probe CMM *Int. J. Adv. Manuf. Technol.* **21** 902–9

[9] Hidaka K 2006 Study of a small-sized ultrasonic probe *Ann. CIRP Manuf. Technol.* **55** 567–70

[10] Sheu D Y 2004 Multi-spherical probe machining by EDM: combining WEDG technology with one-pulse electro-discharge *J. Mater. Process. Technol.* **149** 597–603

[11] Ji H, Hsu H Y, Kong L X and Wedding A B 2009 Development of a contact probe incorporating a Bragg grating strain sensor for nano coordinate measuring machines *Meas. Sci. Technol.* **20** 095304

[12] Fan K C, Hsu H Y, Hung P Y and Wang W L 2006 Experimental study of fabricating a micro ball tip on the optical fiber *J. Opt. A: Pure Appl. Opt.* **8** 782–7

[13] Fan K C, Wang W L and Chiou H S 2008 Fabrication optimization of a micro-spherical fiber probe with the Taguchi method *J. Micromech. Microeng.* **18** 0150111

[14] Shimizu Y, Xu B and Gao W 2012 Fabrication of micro-ball styluses for scanning-type surface form metrology *Int. J. Nanomanufacturing* **8** 87–105

[15] Hogue P and Coopersmith J 2004 Development of an automated optical inspection system for determining percent area coverage for spacecraft contamination control *Proc. SPIE* **5526** 156–63

[16] Fan K C, Chen J Y, Wang C H and Pan W C 2009 Precision *in situ* volume measurement of micro droplets *J. Opt. A: Pure Appl. Opt.* **11** 015503

[17] Zhao X S, Sun T, Tan Y D, Li Z Q and Dong S 2006 Measurement of roundness and sphericity of the micro sphere based on atomic force microscope *Key Eng. Mater.* **315–316** 796–9

[18] Michihata M, Takaya Y and Hayashi T 2008 Development of the nano-probe system based on the laser trapping technique *CIRP Ann.-Manuf. Technol.* **57** 493–6

[19] Michihata M, Takaya Y and Hayashi T 2008 Nano position sensing based on the laser trapping technique for flat surfaces *Meas. Sci. Technol.* **19** 084013

[20] Kühnel M, Ullmann V, Gerhardt U and Manske E 2012 Automated setup for non-tactile high-precision measurements of roundness and cylindricity using two laser interferometers *Meas. Sci. Technol.* **23** 074016

[21] ISO 2011 Geometrical product specifications (GPS)—roundness: part 1. Vocabulary and parameters of roundness *ISO Standards Catalogue* EN ISO 12181-1:2011 (Geneva: ISO)

[22] Reeve C P 1979 Calibration of a roundness standard *National Bureau of Standard* NBSIR 79-1758, USA

[23] Büchner H and Jäger G 2006 A novel plane mirror interferometer without using corner cube reflectors *Meas. Sci. Technol.* **17** 746–52

[24] Fan K C, Lin W L, Chiang L H, Chen S H, Chung T T and Yang Y J 2009 A miniature 2 × 2 mechanical optical switch with a thin MEMS mirror *J. Lightwave Technol.* **27** 1155–61

[25] Cheng F and Fan K C 2011 A linear diffraction grating interferometer with high alignment tolerance and high accuracy *Appl. Opt.* **50** 4550–6

[26] Fan K C, Chu C L and Mou J I 2001 Development of a low-cost autofocusing probe for profile measurement *Meas. Sci. Technol.* **12** 2137–46